Deep-Focus Earthquakes and Recycling of Water into the Earth's Mantle

CHARLES MEADE* AND RAYMOND JEANLOZ

For more than 50 years, observations of earthquakes to depths of 100 to 650 kilometers inside Earth have been enigmatic: at these depths, rocks are expected to deform by ductile flow rather than brittle fracturing or frictional sliding on fault surfaces. Laboratory experiments and detailed calculations of the pressures and temperatures in seismically active subduction zones indicate that this deep-focus seismicity could originate from dehydration and high-pressure structural instabilities occurring in the hydrated part of the lithosphere that sinks into the upper mantle. Thus, seismologists may be mapping the recirculation of water from the oceans back into the deep interior of our planet.

A LARGE NUMBER OF EARTHQUAKES OCCUR WELL BELOW Earth's surface, to depths of 650 km in the mantle (Fig. 1). This deep-focus seismicity originates in the subducted oceanic lithosphere, representing the cold, sinking thermal boundary layer of mantle convection. Observations of these earthquakes have played a fundamental role in the discovery and understanding of plate tectonics (*1*); however, the mechanical origin of these events is still unknown because they occur at depths where high pressures and temperatures should prohibit brittle fracture or frictional sliding on fault surfaces (*2*). The seismic mechanisms that operate under these conditions are of great interest because these earthquakes could provide in situ information about the nature of thermal convection deep in Earth.

Research on this problem has emphasized the possibility that phase transitions may be a source of deep seismicity in the mantle. Melting (*3*), dehydration (*4*), and solid-solid transformations (*5*) have all been invoked. One or more of these processes occur to depths of at least 250 km in subduction zones; however, the evidence that they may produce seismicity has been derived from measurements below 2 GPa, corresponding to depths less than 70 km (for example, *6, 7*). Thus, earlier experiments have not simulated the conditions pertaining to deep-focus earthquakes and, most important, they have not been performed at pressures and temperatures well above the brittle-ductile transition.

To address this problem, we developed techniques for investigating acoustic emissions at high pressures and temperatures in the diamond cell (*8*). Using this approach, which can easily investigate sources of seismicity over the entire range of pressures and temperatures in Earth's mantle, we recently obtained evidence that phase transitions in nongeologic materials at deep mantle pressures can generate shear instabilities and large amounts of acoustic energy (*11*). In this article, we document similar phenomena in hydrous silicates at high pressures and moderate temperatures and suggest that this mechanism could produce deep-focus earthquakes.

Mantle Silicates

We initially studied olivine and its high-pressure phases because they probably make up more then 50% of the subducting slab and the upper mantle (*12*) and because several workers have suggested that deep seismicity may be controlled by the kinetics of the high-pressure phase transformations in these minerals (*6, 13*). Recent observations of sudden shear failure across the Mg_2GeO_4 olivine → γ-spinel transition at 2 GPa have supported this idea (*6*). In general, our results with this material are null findings (*14, 15*) in that we have not observed acoustic emissions upon compression of olivine, with, or without, heating above ~7 GPa (*16*). Specifically, we find that acoustic emissions are not associated with the olivine → spinel, spinel → perovskite + magnesiowüstite or olivine → perovskite + magnesiowüstite transformations in the laser-heated diamond cell. Thus, we find no evidence for the low-pressure failure mechanisms suggested by Green and Burnley (*6*) occurring under the conditions of the silicate olivine → spinel transition in the mantle (*17*). These results are consistent with those of dozens of earlier experiments that have failed to identify any seismic behavior across high-pressure phase transitions in olivine [for example, (*13*)]. Recent high-pressure experiments have documented faults in samples of olivine that have been partially transformed to β-Mg_2SiO_4, however, there is no evidence of seismic behavior associated with these features (*18*).

Similarly, we have not observed acoustic emissions associated with solid-state transformations in pyroxene (for example, to perovskite) (*19*). Thus, we have found no evidence for the release of seismic energy during high-pressure phase transitions of the major, anhydrous mantle phases, even at metastable conditions. Although our experiments cannot rule out the possibility that these transitions could act as seismic sources in Earth, several lines of evidence suggest that this is unlikely. First, it is not evident how these transitions, which occur at discrete depths in mantle, would produce the observed distribution of earthquakes that spans continuously from the surface to approximately 650 km depth (Fig. 1). Moreover, the large volume change associated with the transitions should produce an isotropic component in the seismic focal mechanism, in disagreement with the observations of most deep-focus earthquakes (*20*).

The authors are in the Department of Geology and Geophysics, University of California, Berkeley, CA 94720.

*Present address: Geophysical Laboratory, Carnegie Institution of Washington, 5251 Broad Branch Road, N.W., Washington, DC 20015.

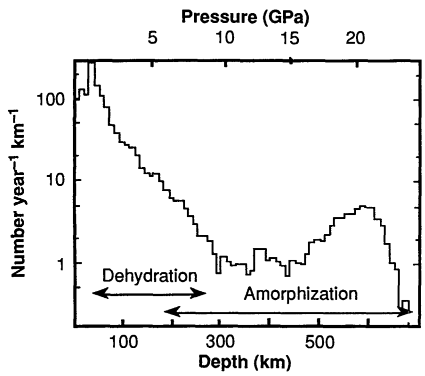

Fig. 1. Distribution of earthquakes with depth in the mantle [after (*20*)]. For comparison, we show the range of pressure at which we observe acoustic emissions during stable (dehydration) and metastable (amorphization) phase transitions in serpentine.

Hydrous Minerals

Recognizing that the suboceanic mantle is hydrothermally altered by the circulation of marine water, as is well documented by studies of ophiolites (*21*), we have examined the mechanical properties of hydrous minerals that are expected to be present in the subducted lithosphere. In particular, we studied serpentine [$(Mg_3Si_2O_5(OH)_4)$], an alteration (hydration) product of olivine and pyroxene that is thought to be an important component of the descending slab (*12, 21*). Earlier experiments have documented brittle failure upon dehydration of serpentine at 0.5 GPa and approximately 950 K, pressures and temperatures that are above the brittle-ductile transition for this mineral (*4*). These observations suggest that dehydration of serpentine could be a source for at least shallow subduction zone earthquakes (<20 km), but the pressure range of this failure mechanism has not been investigated.

Our experiments were performed on a natural serpentine of lizardite structure over a range of pressures (P) and temperatures (T) that brackets the ambient conditions of all subduction zones in the upper mantle ($0 < P < 40$ GPa; $300 < T < 3000$ K). We recorded acoustic emissions associated with two separate structural transformations at high pressures and moderate temperatures (Fig. 2). Similar to the earlier low-pressure experiments, we registered acoustic emissions as serpentine dehydrated between 2 and 9 GPa (Fig. 2). At higher pressures, dehydration does not produce emissions: acoustic emissions were recorded but they were not produced by dehydration, as described below.

In all of our experiments, the dehydration of serpentine could be visually confirmed by a sudden change of color and release of water as the heating laser traversed the sample. Effectively, we are correlating sight and sound in that the acoustic emissions were coincident with the observed progress of the dehydration. We estimate that the dehydration temperatures for our samples, and hence the temperatures for acoustic emissions, were 900 ± 100 K (*22, 23*).

At lower temperatures and higher pressures than those at which we mainly observed dehydration, acoustic emissions occurred over a broad and continuous range of pressure. At room temperature, emissions occurred between 6 and 25 GPa, and they could be audible; in some cases the events could be visually correlated with macroscopic deformation of the sample [compare with (*11, 24*)]. Acoustic emissions were also recorded during laser heating to temperatures less than 900 K at pressures of 6 to 25 GPa (*25*). We confirmed visually that none of the events over this range of pressure and temperature ($6 < P < 25$ GPa; $300 < T < 900$ K) were associated with dehydration of the samples, establishing that they are distinct from the emissions between 2 to 9 GPa, at 900 ± 100 K. Moreover, we conclude that these emissions were not caused by conventional fracturing or frictional sliding on cracks because the shear stresses were a small fraction of the confining pressures [$\sigma \approx$ 0.1 to 1 GPa (*26*)] and because the pressures were at least an order of magnitude above the brittle-ductile transition for serpentine [0.2 to 0.5 GPa at room temperature (*2*)].

X-ray diffraction studies of our samples revealed that the crystal structure of the serpentine was lost over the same pressure interval that we obtained the high-pressure, low-temperature acoustic emissions: that is, for the emissions that were not due to dehydration (Fig. 3). Such crystal → glass transitions are well known for a wide variety of materials, including hydroxides that are compressed metastably at kinetically low temperatures (*23, 27*). Because the temperatures achieved in subduction zones may remain below the dehydration temperature of serpentine until great depth (see below), it is quite likely that serpentine is metastably compressed inside Earth and that it may undergo pressure-induced amorphization within the subducting slab.

The observation that serpentine amorphizes in this manner could have broad implications for the stability of hydrous phases in the subducting lithosphere because a wide range of hydroxy-silicates have similar structures and hence they may exhibit similar behavior under compression (*28*). Indeed, a few initial experiments on talc [$(Mg_6Si_8O_{20}(OH)_4)$] and pyrophyllite [$(Al_4Si_8O_{20}(OH)_4)$] show evidence for acoustic emissions and amorphization at high pressures; these data provide further support for this idea.

Implications for Deep Earthquakes and Recycling of Water into the Mantle

Observations of a wide range of phase transitions have documented acoustic emissions above the brittle-ductile transition that may be similar to the phenomena that we observe in serpentine at both high and low pressures. For example, the emissions associated with dehydration in the diamond cell are probably generated by the same mechanisms as the brittle failure of serpentine with dehydration at ~970 K and 0.5 GPa (*4*). Raleigh and Paterson argued that this temperature-induced brittle deformation (at pressures and temperatures above the conventional brittle-ductile transition) is driven by large increases in pore pressures and hydrolytic weakening associated with dehydration (*29*). Our results suggest that such embrittlement, induced by dehydration, extends up to 9 GPa.

In an earlier study, we documented large acoustic emissions and shear instabilities that were generated by the atomic motions across displacive phase transitions in Si and Ge at pressures well above the brittle-ductile transition (*11*). Similar phenomena are common across martensitic transformations at low pressures (*30*). These events are driven by the shear displacements of atoms during the

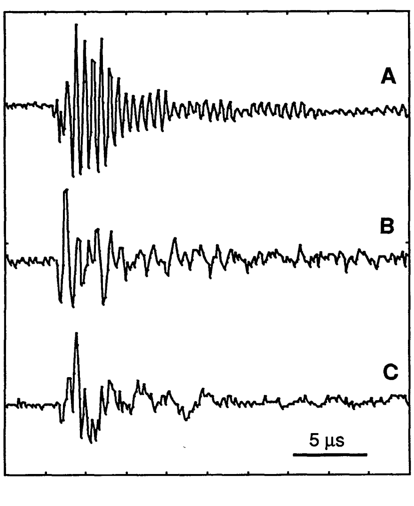

Fig. 2. Acoustic emissions from serpentine samples in the diamond cell detected by a small piezoelectric transducer. (**A**) P = 3 GPa, T = 1080 ± 80 K. The acoustic emission occurred as the sample dehydrated. (**B**) P = 20 GPa, T = 300 K. (**C**) P = 21 GPa, T < 900 ± 100 K (*22*). There is no evidence of dehydration in the events (**B**) and (**C**).

transitions and not by isotropic volume changes. Because the most important prerequisite for this behavior is a diffusionless transformation mechanism, it is likely that the acoustic emissions during the amorphization of serpentine have a similar origin. That is, they are produced by the atomic motions on the scale of the unit cell ($\sim 10^{-10}$ m) as lizardite transforms to a glass. Notably, acoustic emissions are also observed upon recrystallization of glasses (that is, the reverse of our experiments); however, the origin of these events is not well understood (*31*).

Even though our observations were necessarily made on laboratory length-scales, there is evidence that dehydration and amorphization could produce seismicity over geologic dimensions. For example, shallow earthquakes near large reservoirs have been attributed to increased pore pressures along fault surfaces (*32*), analogous to the processes that produce brittle deformation in dehydrated serpentine. Compared to crustal conditions, at which fault zones can be highly permeable, these processes might be enhanced at mantle pressures if pore fluids generated by dehydration are prevented from draining away because of the low permeability of the rock.

Some of the emissions during amorphization result in rapid displacements in parts of the samples over distances of 10^{-5} to 10^{-4} m. This observation indicates that the crystal $\rightarrow$ glass transition can produce shear instabilities that propagate over length-scales at least five orders of magnitude greater than the original source dimension (Fig. 4). Similar shear instabilities have been documented over 10^{-2} m during martensitic transformations at low pressures (*30*); this length is about eight orders of magnitude larger than the unit-cell dimensions at which the transformations are initiated (*33*). In a

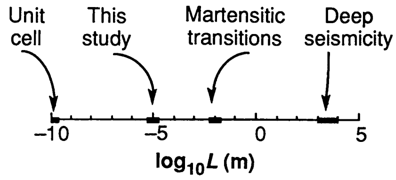

Fig. 4. Length-scales for seismic behavior. The acoustic emissions associated with phase transformations originate on the scale of the unit cell. These emissions reflect shear instabilities that are observed over dimensions of 10^{-5} m in the diamond cell and 10^{-2} m in low-pressure experiments. The range of length-scales inferred from the experiments (eight orders of magnitude) is greater than the difference in scale between the experiments and earthquakes (approximately five orders of magnitude).

similar way, brittle rupture processes are observed over a wide range of scales (*34*). By analogy with the scaling from experimental observations of fracturing to the geologic dimensions of great earthquakes (*35*), we infer that amorphization is also a possible source of seismicity in Earth.

Geologic observations provide qualitative evidence that the mechanisms that produce acoustic emissions in serpentine may also be sources for deep earthquakes in the mantle. In particular, the nearly bimodal distribution of seismicity with depth roughly corresponds to the two pressure intervals of acoustic emissions in the experiments (Fig. 1). Moreover, shallow to intermediate focus earthquakes (30

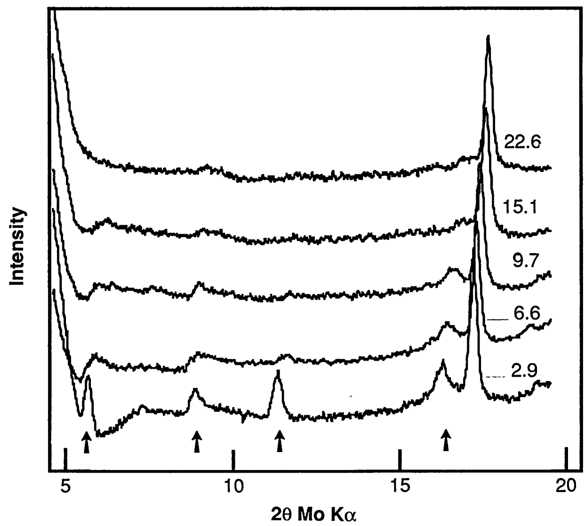

Fig. 3. Powder x-ray diffraction patterns from a sample of lizardite at high pressures and room temperature show that the crystal structure of serpentine is gradually eliminated by compression above 6.6 GPa (*44*). The pressure for each pattern is noted (in gigapaseals). The arrows mark the positions of diffraction peaks from serpentine. The peak at 17° to 18° is the intensity calibration from the gold in the sample. By 22.6 GPa, the diffraction lines of serpentine are barely visible above the background. Such a large decrease in the scattered intensity indicates that crystalline order has been lost; that is, crystalline lizardite has been transformed to a glass at room temperature over a broad range of pressure (6.6 to 22.6 GPa) that coincides with the range of pressure for acoustic emissions ($6 < P < 25$ GPa). Up to 22.6 GPa, this crystal $\rightarrow$ glass transition is reversible because x-ray diffraction on decompressed samples (at $P = 0$) show that lizardite recrystallizes on decreasing pressure. That the amorphization is reversible demonstrates that the transition is driven by changes in pressures and not by shearing of the samples in our experiments. Because the rate of compression was extremely slow in these experiments (over ~ 2 months), we infer that amorphization (and recrystallization) of serpentine will occur for a wide range of pressure-time paths on reasonable laboratory time scales.

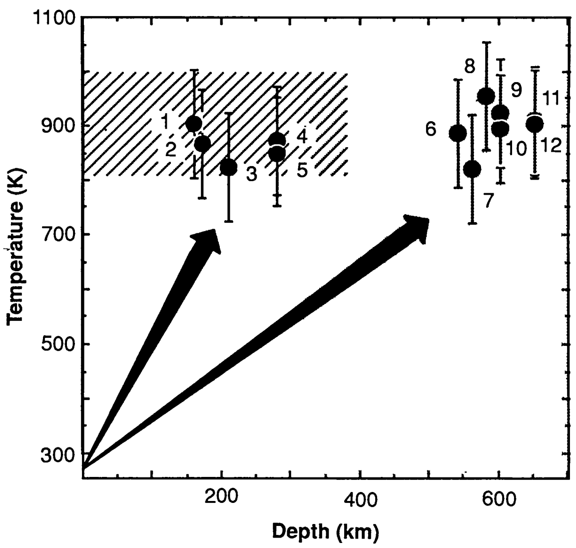

Fig. 5. Minimum temperatures in the upper 12 km of the subducting lithosphere at the maximum depth of observed seismicity for subduction zones throughout the world compared with the range of pressures and temperatures of acoustic emissions in the laboratory (1, Alaska; 2, South Chile; 3, Middle America; 4, Ryuku; 5, Aleutians; 6, Kamchatka; 7, Izu Bonin; 8, Northeast Japan; 9, North Chile; 10, Kuriles; 11, Java; 12, Tonga) (*40*). The arrows show schematic pressure-temperature paths for the coldest material in the upper 12 km of the slabs. The hatched and shaded regions show the pressure-temperature fields for acoustic emissions associated with dehydration ($2 < P < 9$ GPa; $T = 900 \pm 100$ K) and amorphization ($6 < P < 25$ GPa; $300 < T < 900$ K), respectively. Qualitatively similar relations between the minimum temperature and the maximum depth of seismicity have been described in earlier model studies (*39, 41*). We find that the slabs in which seismicity terminates above 300 km are heated to the dehydration temperature of serpentine at the maximum depth of seismicity. In comparison, slabs with the deepest earthquakes are significantly cooler when they pass 300 km; this relation indicates that these slabs may subduct serpentine and other hydroxysilicates to depths below 400 km without dehydration. We emphasize the temperatures in the upper 12 km of the slab, because we assume that this is the deepest level of the hydrothermal alteration beneath the oceanic crust. Deeper into the lithospheric mantle, the slab is cooler (by ~ 50 to 100 K) but the presence of hydrous silicates is uncertain (*21*). The calculations and the laboratory observations suggest that serpentine could not produce seismicity at depths below ~ 650 km, the maximum depth of earthquakes in the mantle (*20*).

to 300 km depth) that would be ascribed to dehydration seem to occur on top of the subducting slab: that is, within the part of the slab where hydrated minerals and sediments are most abundant and are heated first as the lithosphere is thrust down into the mantle (*36*).

Thermal models of subduction zones allow a more quantitative comparison with our experiments because they provide an estimate of the temperature at the observed depths, or pressures of seismicity (*37, 38*). Earlier studies have demonstrated that differences in the seismicity between subduction zones are related to differences in the thermal evolution of the slabs (*39*).

As a specific test, our explanation for subduction zone seismicity suggests that the downgoing lithosphere should have a particular thermal state. First, the slabs with the deepest earthquakes must be cold enough to allow deep subduction of serpentine without dehydration. And second, the termination of seismicity at shallow-intermediate depths should be associated with complete dehydration of the slab.

Detailed thermal calculations of subduction zones are consistent with both of these requirements (Fig. 5) (*40*). For example, in the subduction zones that are seismically active below 300 km, the calculations show that temperatures and pressures within the top 12 km of the slab are comparable to the range of temperatures and pressures where we observe acoustic emissions associated with amorphization of serpentine (*41*). Amorphization may occur in these slabs at these depths because the temperatures in the seismically active parts are below our estimate of the dehydration temperatures for $Mg_3Si_2O_5(OH)_4$ compositions at high pressures (*22*). The calculations also show that slabs with only shallow seismicity are hotter and should be completely dehydrated at their maximum depth of earthquakes (Fig. 5).

Because many slabs retain significant negative buoyancy below their deepest earthquakes, the seismically active parts of the subduction zones provide an incomplete picture of the cold thermal boundary layer for mantle convection. That is, the absence of seismicity below a particular depth does not necessarily mark the end of the slab. From these calculations and our observations, we suggest that the maximum depth of seismicity is controlled by the relation between the pressure-temperature-time history of the descending lithosphere and the (possibly metastable) phase relations of serpentine at high pressures. Thus, the observed distribution of deep-focus earthquakes may illustrate the recycling of water from the surface into the upper mantle.

Further experiments on the focal mechanisms of the acoustic emissions and the stability of hydroxy-silicates at high pressures and temperatures could provide important information on the particular role of serpentine in generating deep-focus earthquakes. Such work would also provide important information on the maximum depth of subduction for hydrous minerals, thereby providing important constraints for quantifying the flux of volatiles between the oceans and mantle. For the present, however, our experiments show that structural transformations in geologic materials can produce seismic energy at pressures and temperatures well above the brittle-ductile transition. In general, this work suggests that large volumes of hydrous minerals may have been subducted into the mantle over geologic time (*42*) and hence that there is an intimate connection between the hydrosphere and the deep mantle of our planet (*43*).

REFERENCES AND NOTES

1. D. L. Turcotte and G. Schubert, *Geodynamics* (Wiley, New York, 1982); D. Gubbins, *Seismology and Plate Tectonics* (Cambridge Univ. Press, Cambridge, 1990).
2. Increasing either pressure or temperature promotes ductile deformation in minerals. For geologic materials inside Earth, the transition between brittle to ductile deformation is at $P \approx 2$ GPa and $T \approx 1000$ K: that is within the upper 70 km of the crust and mantle. See M. S. Paterson, *Experimental Rock Deformation; the Brittle Field* (Springer-Verlag, New York, 1978).
3. D. T. Griggs and J. Handin, *Geol. Soc. Am. Mem.* **79**, 347 (1960).
4. C. B. Raleigh and M. S. Paterson, *J. Geophys. Res.* **70**, 3965 (1965).
5. J. Lomnitz-Adler, *J. Phys. Earth* **38**, 83 (1990).
6. H. W. Green and P. C. Burnley, *Nature* **341**, 733 (1989).
7. S. Kirby, *J. Geophys. Res.* **92**, 13,789 (1987).
8. In all experiments, the samples were contained in either nickel or spring steel gaskets and compressed in a modified Mao-Bell–type diamond cell without a pressure medium. Pressures were measured with the ruby fluorescence technique [H. K. Mao, P. M. Bell, J. W. Shaner, J. Steinberg, *J. App. Phys.* **49**, 3276 (1978)]. Acoustic emissions were recorded with a 500-μm diameter, PZT piezoelectric transducer (100 μm thick, 20-MHz resonant frequency) attached to a pavilion facet of one of the diamond anvils. For experiments at high temperatures, the samples were heated inside the diamond cell by means of a continuous-wave Nd:YAG laser, and the average temperatures were measured by spectroradiometry (*9*).
9. D. L. Heinz and R. Jeanloz, in *High Pressure Research in Mineral Physics*, M. H. Manghnani and Y. Syono, Eds. (American Geophysical Union, Washington, DC, 1987), p. 113.
10. ———, *J. Geophys. Res.* **92**, 11437 (1987).
11. C. Meade and R. Jeanloz, *Nature* **339**, 616 (1989). Audible emissions have been noted either by placing one's ear close to the diamond cell or by recording with a conventional microphone.
12. A. E. Ringwood, *Composition and Petrology of the Earth's Mantle* (McGraw-Hill, New York, 1975); H. S. Yoder, Jr., *Generation of Basaltic Magma* (National Academy of Sciences, Washington, DC, 1976); Basaltic Volcanism Study Project, *Basaltic Volcanism on the Terrestrial Planets* (Pergamon, New York, 1981).
13. C. M. Sung and R. Burns, in *High Pressure Science and Technology*, K. D. Timmerhaus and M. S. Barber, Eds. (Plenum, New York, 1979), vol. 2, pp. 31–42.
14. The starting material for these experiments consisted of San Carlos olivine of composition $(Mg_{0.88},Fe_{0.12})_2SiO_4$, which originates from the upper mantle [R. Jeanloz *et al.*, *Science* **197**, 457 (1977); *J. Geophys. Res.* **85**, 3163 (1980)].
15. For all of the high-temperature experiments, the samples were initially compressed at room temperature before laser-heating. In practice, the maximum pressure is achieved over time scales of 10^2 to 10^3 s. By comparison, the heating occurs extremely rapidly: over time scales much less than 1 s. For the spinel experiments, the olivine was compressed to peak pressures of 14 to 23 GPa. For the perovskite + magnesiowüstite measurements, the samples were compressed to 25 to 35 GPa. When the samples were heated to temperatures between 1000 and 2000 K, the phase transformations could be visually identified by the sudden changes in color as the laser was scanned across the sample (translucent to blue for spinel; translucent or blue to brown and opaque for perovskite + magnesiowüstite). With these techniques, acoustic emissions were not observed as the transformations occurred.
16. The brittle-ductile transition occurs at ~7 GPa at room temperature [C. Meade and R. Jeanloz, *Nature* **348**, 533 (1990); B. Evans and C. Goetze, *J. Geophys. Res.* **84**, 5505 (1979)].
17. A possible explanation for the difference between our experiments and those of Green and Burnley (*6*) is that the observed failure of Mg_2GeO_4 involves brittle processes, which are suppressed at high pressures.
18. H. W. Green, T. E. Young, D. Walker, C. H. Scholz, *Nature* **848**, 720 (1990).
19. The starting material for these experiments consisted of Bamble enstatite of $(Mg_{0.88},Fe_{0.12})SiO_3$ composition [(*10*); E. Knittle and R. Jeanloz, *Science* **235**, 668 (1987)].
20. C. Frohlich, *Annu. Rev. Earth Planet. Sci.* **17**, 250 (1989).
21. Oxygen isotope analyses of ophiolites [R. T. Gregory and H. P. Taylor, Jr., *J. Geophys. Res.* **86**, 2737 (1981)] and orogenic belts [S. W. Wickham and H. P. Taylor, Jr., *Contrib. Mineral. Petrol.* **91**, 122 (1985)] show evidence for hydrothermal circulation to depths >5 km in the suboceanic mantle and ~12 km in the continental crust [see also R. E. Criss and H. P. Taylor, Jr., *Rev. Mineral.* **16**, 227 (1986)]. These results are consistent with the analyses of deep-sea drilling cores which show hydrothermal alteration to the base of the section [~1 km; R. N. Anderson *et al.*, *Nature* **300**, 589 (1982)]. Laboratory experiments suggest that the permeability of rocks should allow hydrothermal circulation of meteoric waters to depths of ~10 to 15 km in relatively cool regions of the oceanic lithosphere [D. L. Smith and B. Evans, *J. Geophys. Res.* **89**, 4125 (1984); L. M. Cathles, *Science* **248**, 323 (1990)]. In addition, magnetotelluric measurements identify a water-rich layer near the top of subducting slabs to depths of 75 to 100 km, indicating that hydrothermal alteration may continue to occur as the lithosphere subducts into the mantle [(R. D. Kurtz *et al.*, *Nature* **321**, 596 (1989); P. E. Wannamaker *et al.*, *J. Geophys. Res.* **94**, 14127 (1989)]. These results are in agreement with stable isotope studies on subduction zone–derived metamorphic rocks [G. E. Bebout, *Science* **251**, 413 (1991)]. In the present study, we assume that the maximumj depth of hydrous alteration is 12 km below the surface of the subducting lithosphere.
22. Experiments on serpentine above 1 GPa suggest a range of dehydration temperatures between 850 to 950 K [for example, K. Yamamoto and S. Akimoto, *Am. J. Sci.* **277**, 288 (1977); B. W. Evans *et al.*, *Scheiz. Min. Pet. Mitt.* **56**, 79 (1976); S. Kitahara *et al.*, *Am. J. Sci.* **264**, 223 (1966); C. Scarfe and P. J. Wyllie, *Nature* **215**, 945 (1967); J. V. Chernosky, *Can. Mineral.* **20**, 19 (1982)]. Within the uncertainty of the measurements, the dehydration temperature of serpentine appears to be approximately invariant with pressure between 2 and 5 GPa, the highest pressures to which the experiments constrain the transition. However, there are large variations in the dehydration temperatures for serpentines of different crystal structure and water content (for example, >100 K between antigorite and chrysotile). Given this range of values and the experimental

uncertainty, we assume that the dehydration temperatures for our samples fall within the range of 900 ± 100 K. Such values are below the temperatures that can be accurately measured by our spectroradiometric system (*9*), although they are entirely compatible with the thermal radiation recorded from our samples.

23. Calculations suggest that the temperatures for equilibrium dehydration reactions in serpentine should decrease with increasing pressure above 3 GPa [J. M. Delany and H. C. Helgeson, *Am. J. Sci.* **278**, 638 (1978)]. Our observations of amorphization in serpentine indicate that these reactions may be kinetically hindered at high pressures and moderate to low temperatures.
24. Because most of these events cannot be corroborated by sight or audible sound we routinely run blank experiments to check that our gaskets and pressure calibrant are seismically quiet at high pressures.
25. Because the acoustic emissions are observed in samples that are laser-heated below the dehydration temperature, we assume that 900 ± 100 K is an upper limit for the temperature of these events (*22*).
26. The shear stresses were determined from measurements of the pressure gradients and samples thicknesses. See C. Meade and R. Jeanloz, *J. Geophys. Res.* **93**, 3261 (1988).
27. Pressure-induced crystal → glass transitions have been documented for a wide variety of crystal structures and bonding types, ranging from SnI_4 and H_2O ice I_h to the quartz and coesite polymorphs of SiO_2, $CaAl_2Si_2O_8$ anorthite, $Ca(OH)_2$ portlandite, $AlPO_4$ berlinite, Fe_2SiO_4 fayalite, and $LiKSO_4$ [Y. Fuji, M. Kowaka, A. Onodera, *J. Phys. C* **18**, 789 (1985); O. Mishima, L. D. Calvert, E. Whalley, *Nature* **310**, 393 (1984); R. J. Hemley, L. C. Chen, H. K. Mao, *ibid.* **338**, 638 (1989); R. J. Hemley, A. P. Jephcoat, H. K. Mao, L. C. Ming, M. Manghnani, *ibid.* **334**, 737 (1988); Q. Williams and R. Jeanloz, *ibid.* **338**, 413 (1989); C. Meade and R. Jeanloz, *Geophys. Res. Lett.* **17**, 1157 (1990); M. Kruger and R. Jeanloz, *Science* **249**, 647 (1990); H. Sankaran, S. K. Sikka, S. M. Sharma, R. Chidambaran, *Phys. Rev. B* **38**, 170 (1988).].
28. For a discussion of the similarities between the structures of hydroxy-silicates see S. W. Bailey, Ed., *Rev. Mineral.* **19** (1988).
29. The acoustic emissions associated with dehydration are probably promoted by the pore pressures of the dehydrated fluids that reduce the effective stress on fault surfaces to a value below the brittle-ductile transition [see M. K. Hubbert and W. W. Rubey, *Bull. Geol. Soc. Am.* **70**, 115 (1959); J. C. Jaeger, *Elasticity, Fracture, and Flow* (Methuen, London, 1969)]. Notably, this failure mechanism is suppressed or reduced in hydroxy silicates that contain smaller amounts of water (for example, talc) (*2*). Although dehydration does not produce acoustic emissions in serpentine above 9 GPa, it is plausible that it could produce seismicity in other hydrous minerals at these pressures.
30. A. Nishiyama, *Martensitic Transformation* (Academic Press, New York, 1978); K. Shimizu and K. Otsuka, in *Shape Memory Effects in Alloys*, J. Perkins, Ed. (Plenum, New York, 1975), pp. 59–87; J. Baram and M. Rosen, *Acta Metall.* **30**, 655 (1982); J. C. Bokros, and E. R. Parker, *ibid.* **11**, 1291 (1963).
31. M. Yamamoto, K. Shirai, M. Yamana, N. Kashiwazaki, N. Watanabe, *Jpn. J. Appl. Phys Lett.* **29**, 1804 (1990).
32. D. W. Simpson, *Annu. Rev. Earth Planet. Sci.* **14**, 21 (1986).
33. The maximum length-scale for this behavior is probably determined by the sample size in the experiments.
34. C. H. Scholz and C. A. Aviles, in *Earthquake Source Mechanics*, S. Das, J. Boatwright, C. H. Scholz, Eds. (American Geophysical Union, Washington, DC, 1986), pp. 147–155.
35. C. H. Scholz, *Mechanics of Earthquakes and Faulting* (Cambridge Univ. Press, Cambridge, 1990).
36. T. Matsuzawa, N. Umino, A. Hasegawa, A. Takagi, *Geophys. J. R. Astron. Soc.* **86**, 767 (1986); E. R. Engdahl and D. Gubbins, *J. Geophys. Res.* **92**, 13,855 (1987).
37. There have been many comparisons between thermal models for subduction zones and the pressures and temperatures for geologic phase transitions [for example, (*22*); P. J. Wyllie, *Geol. Soc. Am. Bull.* **93**, 468 (1982); R. N. Anderson *et al.*, *J. Geol.* **86**, 731 (1978); *ibid.* **88**, 445 (1980); (*38*)].
38. R. Anderson, S. Uyeda, A. Miyashiro, *Geophys. J. R. Astron. Soc.* **44**, 333 (1976).
39. R. Wortel, *Nature* **296**, 553 (1982); D. McKenzie, *Tectonophysics* **10**, 357 (1970); P. Molnar, D. Freedman, J. S. F. Shih, *Geophys. J. R. Astron. Soc.* **56**, 41 (1979).
40. The thermal structures of subduction zones were calculated with a finite-difference computer program that solves the heat-conduction equation for a two-dimensional slab sinking into an isoviscous half-space [J. Brodholt and S. Stein, *Geophys. Res. Lett.* **15**, 1081 (1988); N. Sleep, *Bull. Seismol. Soc. Am.* **63**, 1349 (1973)]. In the model, the slab has an initial conduction geotherm that depends on the age of the slab. As the slab sinks into the half-space, its temperature increases because of thermal conduction and adiabatic compression. To describe the pressure and temperature dependence of the thermal conductivity, we used the model of S. Keiffer [*J. Geophys. Res.* **81**, 3025 (1976)]. The grid spacing for the calculations was ~1.1 km. For the initial ages, lengths, subduction velocities, and dips of seismic zones we used the values given by R. D. Jarrard [*Rev. Geophys. Space Phys.* **24**, 217 (1986)]. We did not include the effects of phase transitions because the latent heats of the olivine → spinel transformation and dehydration reactions probably cancel [compare (*34*); D. Turcotte and G. Schubert, *J. Geophys. Res.* **78**, 5876 (1973); see (*41*).]
41. The temperatures in Fig. 5 are lower than those from earlier calculations. The discrepancy can be traced to a number of assumptions that produce higher temperatures in the old models. Such assumptions include the addition of arbitrary frictional heating terms at the slab-mantle interface, the prescription of constant temperature at the slab-mantle interface, the use of a constant thermal diffusivity with increasing pressure and temperature, and the addition of 135 K throughout the slab and mantle to account for the latent heat of olivine → spinel transformation. Regarding the last point, we estimate that olivine → spinel transformation produces heating of only ~30 K in the cold region of the subduction zone, if one properly accounts for the fraction of olivine and the ambient temperatures present in the slab.
42. If present subduction velocities and plate ages are representative of the past, and applying the volatile budget of S. Peacock [*Science* **248**, 329 (1990)], $\sim 8 \times 10^{20}$ kg of water may have been exchanged between the oceans and mantle over geologic time. This value is more than half of the mass of the present oceans.
43. W. W. Rubey, *Bull. Geol. Soc. Am.* **62**, 1111 (1951).
44. In these experiments, lizardite was mixed with gold (5% by volume) and compressed without a pressure medium in a Mao-Bell diamond cell. The pressures were measured with the ruby fluorescence technique. The x-ray diffraction patterns were recorded on film from a rotating anode Mo-Kα source (λ = 71.073 pm) and they were analyzed with the techniques described by C. Meade and R. Jeanloz [*Rev. Sci. Instrum.* **61**, 2571 (1990)]. We define the beginning of amorphization as the lowest pressure at which the diffracted intensity is significantly reduced (6.6 GPa).
45. We thank L. Finger, H. Helgeson, R. Hemley, C. Prewitt, S. Sacks, and S. Stein for helpful discussion and comments. N. Sleep and S. Stein kindly provided the computer program for calculating subduction zone temperatures. This work was supported by the National Science Foundation and the National Aeronautics and Space Administration.